JACS
JOURNAL OF THE AMERICAN CHEMICAL SOCIETY

Communication

O Kinetic Isotope Effects Reveal an Associative Transition State for Phosphite Dehydrogenase Catalyzed Phosphoryl Transfer

Graeme Howe, and Wilfred A. van der Donk

J. Am. Chem. Soc., **Just Accepted Manuscript** • DOI: 10.1021/jacs.8b06301 • Publication Date (Web): 07 Dec 2018

ACS Publications

is published by the American Chemical Society. 1155 Sixteenth Street N.W., Washington, DC 20036

^{18}O Kinetic Isotope Effects Reveal an Associative Transition State for Phosphite Dehydrogenase Catalyzed Phosphoryl Transfer

Graeme W. Howe*†‡ and Wilfred A. van der Donk*†‡§

† Department of Chemistry, University of Illinois at Urbana-Champaign, 600 South Mathews Avenue, Urbana, Illinois 61801, United States

‡ Carl R. Woese Institute for Genomic Biology, University of Illinois at Urbana-Champaign, 1206 West Gregory Drive, Urbana, Illinois 61801, United States

§ Howard Hughes Medical Institute, University of Illinois at Urbana-Champaign, 1206 West Gregory Drive. Urbana, Illinois 61801, United States

Supporting Information Placeholder

ABSTRACT: Phosphite dehydrogenase (PTDH) catalyzes an unusual phosphoryl transfer reaction in which water displaces a hydride leaving group. Despite extensive effort, it remains unclear whether PTDH catalysis proceeds via an associative or dissociative mechanism. Here, primary ^{2}H and secondary ^{18}O kinetic isotope effects (KIEs) were determined and used together with computation to characterize the transition state (TS) catalyzed by a thermostable PTDH (17X-PTDH). The large, normal ^{18}O KIEs suggest an associative mechanism. Various transition state structures were computed within a model of the enzyme active site and ^{2}H and ^{18}O KIEs were predicted to evaluate the accuracy of each TS. This analysis revealed that 17X-PTDH catalyzes an associative process with little leaving group displacement and extensive nucleophilic participation. This tight TS is likely a consequence of the extremely poor leaving group requiring significant P-O bond formation to expel the hydride. This finding contrasts with the dissociative TS in most phosphoryl transfer reactions from phosphate mono- and diesters.

Phosphite dehydrogenase (PTDH) catalyzes the oxidation of phosphite (PT) to phosphate with the concomitant reduction of NAD^+ to NADH.[1] The enzyme allows microorganisms to use PT as their sole phosphorus source.[2] The favorable thermodynamics (ΔG^o = -15 kcal/mol) and the low cost of PT have attracted attention to PTDH as a cofactor regeneration system.[3,4] This application spurred generation of PTDH mutants with increased activity,[5] thermostability[6] and decreased cofactor specificity to enable regeneration of both NADH and NADPH.[7] These PTDH variants have been used in biocatalytic systems, both as individual regeneration systems and as fusions with monooxygenases within self-sufficient biocatalysts.[8-11] Because PTDH endows organisms with the unique ability to grow on PT, the enzyme has also received attention for biocontainment.[12-15]

Extensive efforts have been made to understand how PTDH displaces an extremely poor leaving group (hydride) with a water nucleophile. Much of this work has focused on a thermostable variant termed 17X-PTDH.[16] All available data suggests that 17X-PTDH and wild type PTDH operate via the same catalytic mechanism.[16,17] His292 is the putative base that activates the water nucleophile and Arg237 is involved in orienting the substrate for catalysis.[1] Other catalytically important residues (Figure 1) were identified by site-directed mutagenesis,[18] crystallography[19] and computation.[20] Pre-steady state kinetics and kinetic isotope effects (KIEs) with deuterated PT have demonstrated that chemistry is entirely rate limiting.[17] While a reasonable mechanism for this process can be postulated from this information (Figure 1), the relative timing of bond-making and bond-breaking and the protonation state of the substrate remain unclear.

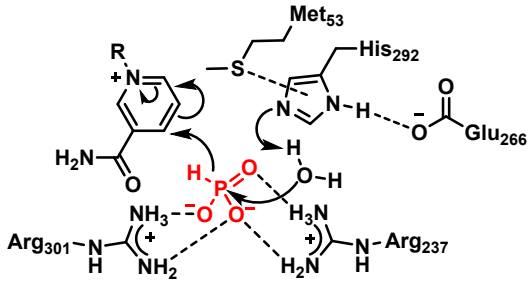

Figure 1. The proposed mechanism of the phosphoryl transfer catalyzed by 17X-PTDH including residues important for catalysis.

Phosphate monoester hydrolyses generally proceed via loose transition states (TSs).[21] However, the chemistry catalyzed by 17X-PTDH is significantly different from a typical phosphoryl transfer. As 17X-PTDH does not accept alternative substrates or nucleophiles,[22] linear free energy relationships (LFERs) cannot be used to probe the TS. Instead, we turned to secondary ^{18}O KIEs ($^{18}(V/K)$). This tool is well-developed for the study of phosphoryl transfer reactions,[21,23] where $^{18}(V/K) > 1$ is expected for a tight TS (significant P-O bond formation, little P-H bond cleavage) and $^{18}(V/K) < 1$ for a loose TS (little bond formation, significant bond cleavage). This interpretation assumes that the dominant contribution to $^{18}(V/K)$ is the difference in P-O bond stretching vibrations in the ground state and the TS (Scheme S1). This framework is an oversimplification and other techniques including computational approaches are required to interpret secondary ^{18}O KIEs confidently and to fully characterize the TS.

Table 1. Steady-state kinetic parameters of 17X-PTDH at various acidities

pH	k_{cat} (s^{-1})	$K_{m,PT}$ (mM)	$K_{m,NAD}$ (mM)	$K_{ia,NAD}$ (mM)	$k_{cat}/K_{m,PT}$ (M^{-1} s^{-1})	^{D}V	$^{D}(V/K)$
5.50	2.4 (0.1)	1.2 (0.1)	0.12 (0.01)	0.8 (0.1)	2.0 (0.2) x 10^3	2.3 (0.2)	2.2 (0.2)
7.25	2.9 (0.6)	0.05 (0.01)	0.033 (0.003)	0.6 (0.2)	6 (2) x 10^4	2.30 (0.04)	2.1 (0.2)
9.00	2.5 (0.6)	0.4 (0.1)	0.06 (0.03)	6 (3)	6 (1) x 10^3	2.29 (0.07)	2.1 (0.2)

Steady-state kinetic parameters of 17X-PTDH were determined from the initial rates of NADH production at varying concentrations of NAD^+ and PT (Table 1; Figure S1). The primary H/D KIEs on V_{max} (^{D}V) and $k_{cat}/K_{m,PT}$ ($^{D}(V/K)$) were determined by direct comparison of the values obtained with protiated and deuterated PT (Figure S2). The dependence of $k_{cat}/K_{M,PT}$ on pH and the independence of ^{D}V with varying acidity agree with previously reported data.[16]

Values of $^{18}(V/K)$ were determined using NMR spectroscopy as described by Bennet.[24] ^{18}O-labeled PT was prepared by hydrolyzing PCl_3 with $H_2{}^{18}O$.[25] The effect per ^{18}O on the ^{31}P chemical shift ($\Delta\delta \sim 0.03$ ppm) allowed quantification of the isotopic composition by spectral deconvolution (Figure 2a). The initial isotopic composition (R_0) of a mixture of $^{18}O_3$-PT and $^{16}O_3$-PT was determined from the relative peak areas of each isotopologue. After the addition of 17X-PTDH, ^{31}P NMR spectra were recorded over time. The ratio of $^{18}O_3$-PT to $^{16}O_3$-PT (R) was determined as a function of the fractional conversion of the light isotopologue (F_1) and fit to Equation 1.[26] A subset of spectra from one experiment and the corresponding fit to Equation 1 are shown in Figure 2.

$$\frac{R}{R_0} = (1 - F_1)^{\left(\frac{1}{\mathrm{KIE}}\right) - 1} \qquad (eq\ 1)$$

$^{18}(V/K)$ was determined at different acidities (Figures S3-S5). In all cases, $^{18}(V/K)$ was large and normal (Table 2). The variation with pH might suggest changes in the TS but this is inconsistent with the constant ^{D}V across the pH range. As the protonation state of PT ($pK_a^2 = 6.62$) changes across this pH range, an equilibrium isotope effect (EIE) on the pK_a of the labeled PT likely contributes to the observed $^{18}(V/K)$. We determined this EIE by monitoring the chemical shift of each isotopologue as a function of pH (Figure S6).[27] The obtained EIE of 1.016 ± 0.001 was in excellent agreement with reported EIEs on the second pK_a of phosphate.[28]

The EIE enriches the dianionic PT in ^{16}O. If 17X-PTDH binds dianionic PT (Scheme S2), the "active" substrate pool would be enriched in the light isotopologue, resulting in a normal contribution to the observed $^{18}(V/K)$. Dividing the KIEs observed at each acidity by the appropriate portion of the EIE (as determined by the percent of PT present as the dianion at each pH; see Supporting Information)[29] results in a pH independent ^{18}O KIE of 1.017 ± 0.001 (Table 2). Conversely, if 17X-PTDH binds monoanionic PT (Scheme S2), the active substrate would be enriched in ^{18}O and the EIE would inversely contribute to the observed $^{18}(V/K)$. Multiplying each observed KIE by the appropriate portion of the EIE gives a pH independent ^{18}O KIE of 1.031 ± 0.001 for monoanionic PT (Table 2). Regardless of which substrate protonation state is correct, these values (1.017 and 1.031) are both large, normal KIEs.

To facilitate interpretation of the observed KIEs, TSs for the 17X-PTDH-catalyzed reaction were computed within a model of the active site. Such analysis typically requires determination of the intrinsic KIEs.[30-33] However, it has been demonstrated that chemistry is entirely rate-limiting for 17X-PTDH and the observed ^{D}V is the intrinsic KIE (^{D}k).[17] Since ^{D}V and $^{D}(V/K)$ are essentially identical (Table 1), a significant forward commitment factor (c_f) is unlikely and the $^{18}(V/K)$ will reflect the intrinsic KIE (^{18}k; eq 2).[34]

$$^{18}(V/K) = \frac{^{18}k + c_f}{1 + c_f} \qquad (eq\ 2)$$

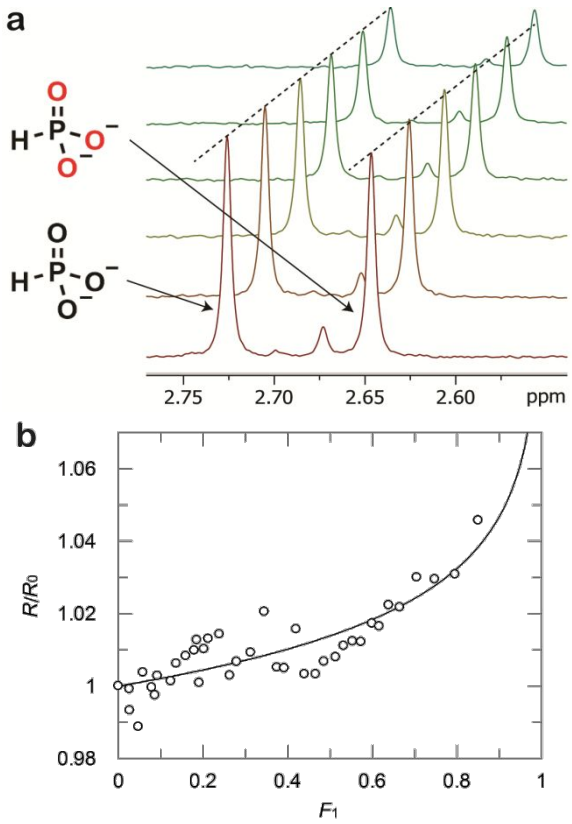

Figure 2. $^{18}O/^{16}O$ ratios determined by ^{31}P NMR spectroscopy during 17X-PTDH catalysis at pH 7.25. (a) A subset of ^{31}P NMR spectra illustrating accumulation of the $^{18}O_3$ isotopologue as the reaction progresses. (b) $^{18}(V/K)$ was obtained by fitting R/R_0 ratios at various fractional conversions (F_1) to eq 1.

Table 2. Observed and corrected secondary ^{18}O KIEs for the 17X-PTDH catalyzed reaction

pH	Measured $^{18}(V/K)^a$	Average $^{18}(V/K)^b$	$^{18}(V/K)$ for monoanionic PT[c]	$^{18}(V/K)$ for dianantionic PT[c]
5.50	1.031 (1) 1.030 (2) 1.031 (2)	1.031 (1)	1.031 (1)	1.017 (1)
7.25	1.020 (1) 1.021 (1) 1.019 (1)	1.020 (1)	1.031 (1)	1.017 (1)
9.00	1.018 (1) 1.017 (2) 1.016 (1)	1.017 (1)	1.031 (1)	1.017 (1)

[a]Determined by fitting R/R_0 and F_1 to eq 1. Errors are from curve fitting. [b]Errors are standard deviations from triplicate measurements. [c]KIEs corrected for the EIE on the protonation state of PT (see Supporting Information).

A TS for the reaction of monoanionic PT was located using the M06-2X/6-31G* level of theory as implemented in Gaussian 09.[35] Solvation effects were considered with the polarizable continuum model.[36,37] This structure exhibited significant P-O_{nuc} bond formation and little P-H bond cleavage. Next, P-O_{nuc} (d1; Figure 3a) and P-H (d2; Figure 3a) bond distances were altered by 0.05 Å intervals and additional TSs were identified with these distances fixed. KIEs were computed for each structure using ISOEFF07 (Figure 3b).[38] Structures with d2 = 1.580 Å gave ^{2}H KIEs in good agreement with the observed value. With d1 = 1.841 Å, the calculated ^{18}O KIE matched the expected value for monoanionic PT. No TSs could be found that predicted ^{18}O KIEs as large as 1.031. TSs located with dianionic PT predicted inverse ^{18}O KIEs. Collectively, these results suggest a mechanism in which dianionic PT binds to 17X-PTDH with His292 protonated. Then, proton transfer occurs in the ternary complex before phosphoryl transfer from monoanionic PT (Scheme 1) that proceeds through a tight TS (Figure 3a) with bond orders of 0.75 for the P-O bond and 0.70 for the P-H bond. Chemistry occurring on the monoanionic substrate is satisfying since it resembles a phosphate diester from which phosphoryl transfers proceed through less dissociative mechanisms than phosphate monoesters.[21] Calculations used to arrive at this structure were relatively insensitive to the basis set used (Tables S6 – S10).

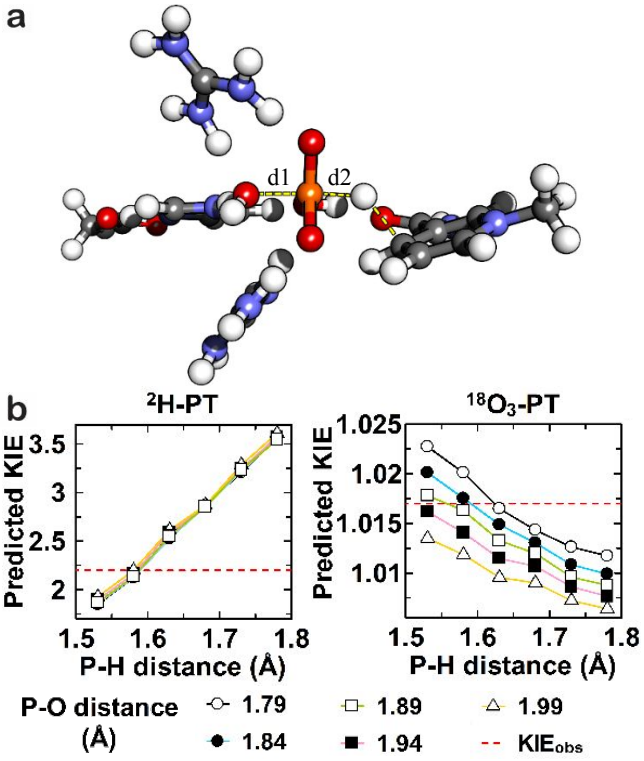

Figure 3. (a) TS model for the 17X-PTDH-catalyzed reaction with monoanionic PT. (b) Predicted KIEs at various P-H and P-O bond lengths. Dashed red lines represent experimental KIEs.

Scheme 1. 17X-PTDH binds dianionic PT with protonated His292. Proton transfer from His292 to PT precedes the phosphoryl transfer from the monoanionic PT.

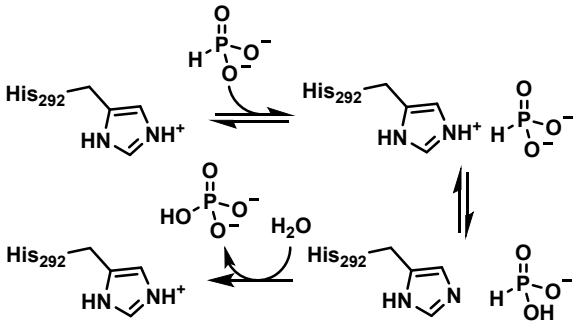

The protonation of dianionic PT by His292 upon binding could be part of a binding isotope effect (BIE) that would inversely contribute to $^{18}(V/K)$.[28,39] That contribution may or may not be counteracted by other interactions in the ternary complex. While BIEs can be normal or inverse, 17X-PTDH would likely constrain the vibrational state of the oxygen atoms of PT.[40] Since this potential inverse contribution of substrate binding is not accounted for by our model, we posit that $^{18}(V/K)$ of 1.017 reflects the lower limit of ^{18}k suggesting a P-O bond length of < 1.89 Å in the TS (Figure 3b). As ^{D}V accurately reflects ^{D}k, the P-H bond length in the TS will be approximately 1.59 Å (for discussion of potential tunneling, see the Supporting Information).

Additional calculations were performed to evaluate the influence of the arginine mimics on the TS geometry and KIEs. Removal of the guanidinium ions did not significantly alter the tightness of the TS (Table S5). This finding is consistent with the observation that positive charges common to the active site of phosphotransferases do not promote tightening of the TS.[21,41-43] In the presence of the arginine mimics, the predicted ^{18}O KIEs are smaller (Table S5). This decrease results from the nonbridging oxygen atoms becoming more vibrationally restricted when interacting with the guanidinium ions. As both Arg237 and Arg301 are known to be important for 17X-PTDH catalysis and are in the active site,[16,18] the model that includes two guanidinium ions better reflects the enzymatic reaction. TSs located within this model suggest the arginine residues orient the substrate for catalysis and activate the nucleophilic water for deprotonation. These calculations also predict a significantly larger activation barrier in the absence of the arginine mimics (Table S5), consistent with the drastic reduction in activity upon mutation of either catalytic arginine.[16,18]

Compared to the loose TSs observed for phosphate monoester hydrolyses, the TS proposed for 17X-PTDH catalysis is consistent with an expected anti-Hammond effect due to the significantly worse leaving group.[21,44] On a More-O'Ferrall-Jencks plot[45,46] for P-O bond formation and cleavage of the bond to a generic leaving group, the change from alkoxide to hydride as leaving group will raise the energy of the metaphosphate corner (Figure S7). Consequently, the TS will shift towards the phosphorane corner, leading to more P-O bond formation and less bond cleavage to the leaving group, which we observe. The upper-right corner of this plot would also increase in energy with a hydride leaving group. The resulting Hammond effect would shift the TS towards the products. If both effects were equal in importance, the net effect would predict increased P-O bonding to the incoming nucleophile and little difference in the extent of leaving group departure (Figure S7). Our proposed TS shows little evidence for this Hammond effect, which could reflect the extremely exergonic nature of the 17X-PTDH reaction or an imbalance in the magnitude of the Hammond and anti-Hammond effects (Figure S7).

The large, normal $^{18}(V/K)$ reported here for 17X-PTDH catalysis is similar to observations for phosphate triester hydrolyses,[21,47] which proceed via tight TSs. Supplementing the data with computation provides a TS structure that is consistent with the observed H/D and ^{18}O KIEs. This structure illustrates a tighter TS than would be expected for the hydrolysis of phosphate mono- and diesters and provides the first insights into the TS for the unusual phosphoryl transfer catalyzed by PTDH.

ASSOCIATED CONTENT

Supporting Information

The Supporting Information is available free of charge on the ACS Publications website.

Full citation for reference 33; experimental procedures; $^{18}(V/K)$ data sets; Cartesian coordinates and thermodynamics of computed structures; computational methodology; discussions on commitment factors, binding isotope effects and hydride tunneling.

AUTHOR INFORMATION

Corresponding Authors

*Phone: (217) 244-5360. Fax: (217) 244-8068. E-mail: vddonk@illinois.edu.

*E-mail: gwhowe@illinois.edu

Notes

The authors declare no competing financial interests.

ACKNOWLEDGMENTS

We thank X. Guan and L. Zhu for assistance with NMR data acquisition, and D. Herschlag for helpful discussions. Data were collected on a 600 MHz NMR funded by NIH S10-RR028833. GWH is the recipient of an NSERC Postdoctoral Fellowship. This work was supported by the Howard Hughes Medical Institute.

REFERENCES

(1) Vrtis, J. M.; White, A. K.; Metcalf, W. W.; van der Donk, W. A. *J. Am. Chem. Soc.* Phosphite Dehydrogenase: An Unusual Phosphoryl Transfer Reaction. **2001**, *123*, 2672.

(2) Costas, A. M. G.; White, A. K.; Metcalf, W. W. Purification and Characterization of a Novel Phosphorus-oxidizing Enzyme from Pseudomonas stutzeri WM88. *J. Biol. Chem.* **2001**, *276*, 17429.

(3) Vrtis, J. M.; White, A. K.; Metcalf, W. W.; van der Donk, W. A. Phosphite Dehydrogenase: A Versatile Cofactor-Regeneration Enzyme. *Angew. Chem. Int. Ed.* **2002**, *41*, 3257.

(4) van der Donk, W. A.; Zhao, H. Recent developments in pyridine nucleotide regeneration. *Curr. Opin. Biotechnol.* **2003**, *14*, 421.

(5) Woodyer, R.; van der Donk, W. A.; Zhao, H. Optimizing a Biocatalyst for Improved NAD(P)H Regeneration: Directed Evolution of Phosphite Dehydrogenase. *Comb. Chem. High Throughput Screening* **2006**, *9*, 237.

(6) Johannes, T. W.; Woodyer, R. W.; Zhao, H. Directed Evolution of a Thermostable Phosphite Dehydrogenase for NAD(P)H Regeneration. *Appl. Environ. Microbiol.* **2005**, *71*, 5728.

(7) Woodyer, R.; van der Donk, W. A.; Zhao, H. Relaxing the Nicotinamide Cofactor Specificity of Phosphite Dehydrogenase by Rational Design. *Biochemistry* **2003**, *42*, 11604.

(8) Torres Pazmino, D. E.; Snajdrova, R.; Baas, B. J.; Ghobrial, M.; Mihovilovic, M. D.; Fraaije, M. W. Self-Sufficient Baeyer-Villiger Monooxygenases: Effective Coenzyme Regeneration for Biooxygenation by Fusion Engineering. *Angew. Chem. Int. Ed.* **2008**, *47*, 2275.

(9) Krauser, S.; Hoffmann, T.; Heinzle, E. Directed Multistep Biocatalysis for the Synthesis of Polyketide Oxytetracycline in Permeabilized Cells of Escherichia coli. *ACS Catal.* **2015**, *5*, 1407.

(10) Messiha, H. L.; Ahmed, S. T.; Karuppiah, V.; Suardiaz, R.; Ascue Avalos, G. A.; Fey, N.; Yeates, S.; Toogood, H. S.; Mulholland, A. J.; Scrutton, N. S. Biocatalytic Routes to Lactone Monomers for Polymer Production. *Biochemistry* **2018**, *57*, 1997.

(11) Beyer, N.; Kulig, J. K.; Fraaije, M. W.; Hayes, M. A.; Janssen, D. B. Exploring PTDH-P450BM3 Variants for the Synthesis of Drug Metabolites. *ChemBioChem* **2018**, *19*, 326.

(12) Shaw, A. J.; Lam, F. H.; Hamilton, M.; Consiglio, A.; MacEwen, K.; Brevnova, E. E.; Greenhagen, E.; LaTouf, W. G.; South, C. R.; van Dijken, H.; Stephanopoulos, G. Metabolic engineering of microbial competitive advantage for industrial fermentation processes. *Science* **2016**, *353*, 583.

(13) Hirota, R.; Abe, K.; Katsuura, Z.; Noguchi, R.; Moribe, S.; Motomura, K.; Ishida, T.; Alexandrov, M.; Funabashi, H.; Ikeda, T.; Kuroda, A. A Novel Biocontainment Strategy Makes Bacterial Growth and Survival Dependent on Phosphite. *Sci. Rep.* **2017**, *7*, 44748.

(14) Pandeya, D.; López-Arredondo, D. L.; Janga, M. R.; Campbell, L. M.; Estrella-Hernández, P.; Bagavathiannan, M. V.; Herrera-Estrella, L.; Rathore, K. S. Selective fertilization with phosphite allows unhindered growth of cotton plants expressing the ptxD gene while suppressing weeds. *Proc. Natl Acad. Sci. U. S. A.* **2018**, *115*, E6946.

(15) Motomura, K.; Sano, K.; Watanabe, S.; Kanbara, A.; Nasser, A. G.; Ikeda, T.; Ishida, T.; Funabashi, H.; Kuroda, A.; Hirota, R. Synthetic Phosphorus Metabolic Pathway for Biosafety and Contamination Management of Cyanobacterial Cultivation. *ACS Synth. Biol.* **2018**, *7*, 2189.

(16) Hung, J. E.; Fogle, E. J.; Christman, H. D.; Johannes, T. W.; Zhao, H.; Metcalf, W. W.; van der Donk, W. A. Investigation of the Role of Arg301 Identified in the X-ray Structure of Phosphite Dehydrogenase. *Biochemistry* **2012**, *51*, 4254.

(17) Fogle, E. J.; van der Donk, W. A. Pre-Steady-State Studies of Phosphite Dehydrogenase Demonstrate That Hydride Transfer Is Fully Rate Limiting. *Biochemistry* **2007**, *46*, 13101.

(18) Woodyer, R.; Wheatley, J. L.; Relyea, H. A.; Rimkus, S.; van der Donk, W. A. Site-Directed Mutagenesis of Active Site Residues of Phosphite Dehydrogenase. *Biochemistry* **2005**, *44*, 4765.

(19) Zou, Y.; Zhang, H.; Brunzelle, J. S.; Johannes, T. W.; Woodyer, R.; Hung, J. E.; Nair, N.; van der Donk, W. A.; Zhao, H. M.; Nair, S. K. Crystal Structures of Phosphite Dehydrogenase Provide Insights into Nicotinamide Cofactor Regeneration. *Biochemistry* **2012**, *51*, 4263.

(20) Ranaghan, K. E.; Hung, J. E.; Bartlett, G. J.; Mooibroek, T. J.; Harvey, J. N.; Woolfson, D. N.; van der Donk, W. A.; Mulholland, A. J. A catalytic role for methionine revealed by a combination of computation and experiments on phosphite dehydrogenase. *Chem. Sci.* **2014**, *5*, 2191.

(21) Lassila, J. K.; Zatalan, J. G.; Herschlag, D. Biological Phosphoryl-Transfer Reactions: Understanding Mechanism and Catalysis. *Annu. Rev. Biochem.* **2011**, *80*, 669.

(22) Relyea, H. A.; Vrtis, J. M.; Woodyer, R.; Rimkus, S. A.; van der Donk, W. A. Inhibition and pH Dependence of Phosphite Dehydrogenase. *Biochemistry* **2005**, *44*, 6640.

(23) Cleland, W. W. Secondary ^{18}O isotope effects as a toole for studying reactions of phosphate mono-, di-, and triesters. *FASEB J.* **1990**, *4*, 2899.

(24) Chan, J.; Lewis, A. R.; Gilbert, M.; Karwaski, M. F.; Bennet, A. J. A Direct NMR Method for the Measurement of Competitive Kinetic Isotope Effects. *Nat. Chem. Biol.* **2010**, *6*, 405.

(25) Carrington, S. J.; Buckingham, D. A.; Simpson, J.; Blackman, A. G.; Clark, C. R. Reactivity of free and Co(III)-coordinated phosphite; Mechanisms of bromine oxidation and H/D exchange. *J. Chem. Soc., Dalton Trans.* **1999**, 3809.

(26) Melander, L.; Saunders, W. H., Jr. *Reaction rates of isotopic molecules.* Robert E. Krieger Publishing: Malabar, FL, 1987.

(27) Ellison, L. R.; Robinson, M. J. T. A Precise N.M.R. Method for Measuring Isotope Effects on Acid-Base Equilibria: Effects of Solvent, Solvent Isotopic Composition, and Ionic Strength on Hydrogen and Oxygen Isotope Effects in Formic Acid. *J. Chem. Soc., Chem. Commun.* **1983**, 745.

(28) Knight, W. B.; Weiss, P. M.; Cleland, W. W. Determination of Equilibrium ^{18}O Isotope Effects on the Deprotonation of Phosphate and Phosphate Esters and the Anomeric Effect on Deprotonation of Glucose 6-Phosphate. *J. Am. Chem. Soc.* **1986**, *108*, 2759.

(29) Weiss, P. M.; Cleland, W. W. Alkaline Phosphatase Catalyzes the Hydrolysis of Glucose 6-Phosphate via a Dissociative Mechanism. *J. Am. Chem. Soc.* **1989**, *111*, 1928.

(30) Moggré, G. J.; Poulin, M. B.; Tyler, P. C.; Schramm, V. L.; Parker, E. J. Transition State Analysis of Adenosine Triphosphate Phosphoribosyltransferase. *ACS Chem. Biol.* **2017**, *12*, 2662.

(31) Firestone, R. S.; Schramm, V. L. The Transition-State Structure for Human MAT2A from Isotope Effects. *J. Am. Chem. Soc.* **2017**, *139*, 13754.

(32) Ducati, R. G.; Firestone, R. S.; Schramm, V. L. Kinetic Isotope Effects and Transition State Structure for Hypoxanthine-Guanine-Xanthine Phosphoribosyltransferase from Plasmodium falciparum. *Biochemistry* **2017**, *56*, 6368.

(33) Poulin, M. B.; Schneck, J. L.; Matico, R. E.; McDevitt, P. J.; Huddleston, M. J.; Hou, W.; Johnson, N. W.; Thrall, S. H.; Meek, T. D.; Schramm, V. L. Transition State for the NSD2-catalyzed Methylation of Histone H3 Lysine 36. *Proc. Natl. Acad. Sci. U. S. A.* **2016**, *113*, 1197.
(34) Cook, P. F.; Cleland, W. W. *Enzyme Kinetics and Mechanism.* Garland Science: New York, NY, 2007.
(35) Frisch, M. J.; et al. *Gaussian 09*, Gaussian, Inc.: Wallingford, CT, 2009.
(36) Tomasi, J.; Persico, M. Molecular Interaction in Solution: An Overview of Methods Based on Continuous Distributions of the Solvent. *Chem. Rev.* **1994**, *94*, 2027.
(37) Scalmani, G.; Frisch, M. J. Continuous Surface Charge Polarizable Continuum Models of Solvation. I. General Formalism. *J. Chem. Phys.* **2010**, *132*, 114110.
(38) Anisinov, V.; Paneth, P. ISOEFF07. Technical University of Lodz: Lodz, Poland, 2007.
(39) Schramm, V. L. Binding isotope effects: boon and bane. *Curr. Opin. Chem. Biol.* **2007**, *11*, 529.
(40) Roston, D.; Cui, Q. Substrate and Transition State Binding in Alkaline Phosphatase Analyzed by Computation of Oxygen Isotope Effects. *J. Am. Chem. Soc.* **2016**, *138*, 11946.
(41) O'Brien, P. J.; Herschlag, D. Does the Active Site Arginine Change the Nature of the Transition State for Alkaline Phosphatase-Catalyzed Phosphoryl Transfer? *J. Am. Chem. Soc.* **1999**, *121*, 11022.
(42) Zatalan, J. G.; Herschlag, D. Alkaline Phosphatase Mono- and Diesterase Reactions: Comparative Transition State Analysis. *J. Am. Chem. Soc.* **2006**, *128*, 1293.
(43) McWhirter, C.; Lund, E. A.; Tanifum, E. A.; Feng, G.; Sheikh, Q. I.; Hengge, A. C.; Williams, N. H. Mechanistic Study of Protein Phosphatase-1 (PP1), A Catalytically Promiscuous Enzyme. *J. Am. Chem. Soc.* **2008**, *130*, 13673.
(44) Herschlag, D.; Jencks, W. P. Evidence that metaphosphate monoanion is not an intermediate in solvolysis reactions in aqueous solution. *J. Am. Chem. Soc.* **1989**, *111*, 7579.
(45) More O'Ferrall, R. A. Relationships between E2 and E1cb Mechanisms of Beta-Elimination. *J. Chem. Soc. B* **1970**, 274.
(46) Jencks, W. P. General acid-base catalysis of complex reactions in water. *Chem. Rev.* **1972**, *72*, 705.
(47) Caldwell, S. R.; Raushel, F. M.; Weiss, P. M.; Cleland, W. W. Transition-state structures for enzymatic and alkaline phosphotriester hydrolysis. *Biochemistry* **1991**, *30*, 7444.

Table of Contents artwork